Perfect chemomechanical coupling of F_oF_1-ATP synthase

Naoki Soga[a,1], Kazuya Kimura[a], Kazuhiko Kinosita Jr.[a], Masasuke Yoshida[b], and Toshiharu Suzuki[a,b,1,2]

[a]Department of Physics, Faculty of Science and Engineering, Waseda University, Tokyo 169-8555, Japan; and [b]Department of Molecular Bioscience, Kyoto Sangyo University, Kyoto 603-8555, Japan

Edited by Pierre A. Joliot, Institut de Biologie Physico-Chimique, Paris, France, and approved April 4, 2017 (received for review January 20, 2017)

F_oF_1-ATP synthase (F_oF_1) couples H^+ flow in F_o domain and ATP synthesis/hydrolysis in F_1 domain through rotation of the central rotor shaft, and the H^+/ATP ratio is crucial to understand the coupling mechanism and energy yield in cells. Although H^+/ATP ratio of the perfectly coupling enzyme can be predicted from the copy number of catalytic β subunits and that of H^+ binding *c* subunits as *c*/β, the actual H^+/ATP ratio can vary depending on coupling efficiency. Here, we report actual H^+/ATP ratio of thermophilic *Bacillus* F_oF_1, whose *c*/β is 10/3. Proteoliposomes reconstituted with the F_oF_1 were energized with ΔpH and Δψ by the acid–base transition and by valinomycin-mediated diffusion potential of K^+ under various [ATP]/([ADP]·[Pi]) conditions, and the initial rate of ATP synthesis/hydrolysis was measured. Analyses of thermodynamically equilibrated states, where net ATP synthesis/hydrolysis is zero, show linear correlation between the chemical potential of ATP synthesis/hydrolysis and the proton motive force, giving the slope of the linear function, that is, H^+/ATP ratio, 3.3 ± 0.1. This value agrees well with the *c*/β ratio. Thus, chemomechanical coupling between F_o and F_1 is perfect.

F_oF_1-ATP synthase | chemiosmotic coupling theory | ATPase | proton motive force | electrochemical potential

Most of cellular ATP is provided by F_oF_1-ATP synthase (F_oF_1) that is located in bacterial membranes, inner membranes of mitochondria, and thylakoid membrane of chloroplast. It synthesizes ATP from ADP and inorganic phosphate (Pi) by the energy of H^+ flow driven by proton motive force (*pmf*) across membranes (1–4). The enzyme is composed of two rotary motors, membrane-peripheral F_1 and membrane-embedded F_o. The simplest version of F_oF_1 is found in bacteria where subunit composition of F_1 is $\alpha_3\beta_3\gamma\delta\varepsilon$ and that of F_o is ab_2c_x (*x* is variable among species). In F_1 motor, γε rotates against a stator part, $\alpha_3\beta_3\delta$-ring by the energy of ATP hydrolysis (5). It also catalyzes reverse reaction, ATP synthesis, when the rotor is forced to rotate in the opposite direction (6, 7). F_o motor is driven by H^+ flow, where a *c* ring formed by multimeric *c* subunits rotates as a rotor relative to the stator, ab_2. Because stators and rotors of the two motors are respectively connected in the whole F_oF_1 architecture, F_oF_1 achieves energy conversion between *pmf* and chemical potential of ATP hydrolysis/synthesis via rotation, the direction of which is determined by the balance of the two energies.

The number of protons moving across membranes coupled with a single ATP synthesis/hydrolysis, defined as H^+/ATP ratio, is crucial to understand not only the coupling mechanism of F_oF_1 but also the energy balance of cells. During one revolution of the motor, each of three catalytic β subunits in F_1 synthesizes/hydrolyzes one ATP molecule, and each of the *c* subunits in *c* ring of F_o transports one proton. Therefore, if the coupling is perfect, the H^+/ATP ratio is determined by the stoichiometric ratio of *c* subunits per β-subunits in F_oF_1, *c*/β. The number of *c* subunits in the *c* ring is dependent on the species: 14 of spinach chloroplast (8, 9), 8 of bovine (10), and 10 of yeast mitochondria (11), thermophilic *Bacillus* PS3 (12), and *Escherichia coli* (13). The approximate *c*/β value is 4.7 for chloroplast, 2.7 for bovine, and 3.3 for yeast, *E. coli*, and *Bacillus* PS3. However, reported values of H^+/ATP ratios are 4.0 ± 0.3 of chloroplast (14), 2.9 ± 0.2 of yeast (15), and 4.0 ± 0.3 of *E. coli* (16). The ratios obtained experimentally were similar to but different from their theoretical values, all of which were outside error limit of the experimental values, although the ratios were roughly correlated to the multimeric numbers of *c* rings. The reason for the disagreement may be intrinsic, such as slippage of the motor, activation of the inactive F_oF_1, and leak of protons, or may be related to insufficient accuracy of measurements. Recently, we have developed a reconstituted proteoliposome (PL) system for thermophile F_oF_1 (TF_oF_1) from *Bacillus* PS3 that shows a reasonable rate of ATP synthesis/hydrolysis at room temperature with high stability and reproducibility (17). The improved experimental procedures of the system include a simple preparation of stable PLs, and extensive removal of contaminating K^+ from phospholipids and of ATP from ADP preparations. In this report, we used this system to determine the actual H^+/ATP ratio. The results show the perfect agreement of H^+/ATP ratio to *c*/β, indicating tight coupling efficiency of proton translocation in F_o and ATP synthesis/hydrolysis in F_1. In addition, kinetic and energetic equivalence of transmembrane difference of pH (ΔpH) and electric potential (Δψ) was supported with unprecedented certainty over a wide range of *pmf* values.

Results

ATP Synthesis/Hydrolysis by TF_oF_1 Under Varying *pmf*. We imposed *pmf* of varying magnitude across membranes of PLs in the presence of 80 μM ADP, 10 mM Pi, and 512 nM ATP, and measured the initial rates of ATP synthesis/hydrolysis catalyzed by TF_oF_1. The rates were plotted against *pmf*, and the pmf_{eq} value where no net catalysis occurred (the rate was zero) was obtained from interpolation of the rate-vs.-*pmf* plots (Fig. 1). At the point of pmf_{eq}, $K_{(ATP)}$ (= [ATP]/[ADP]·[P_i]) corresponds to an equilibrium constant, $K_{(ATP)eq}$. In the experiments, PLs were equilibrated in the

Significance

Peter D. Mitchell, a Nobel awardee in 1978, proposed that F_oF_1-ATP synthase converts energy between electrochemical potential of H^+ across biological membrane ($\Delta\tilde{\mu}_{H^+}$), which is established by respiratory chain complexes, and chemical potential of adenine nucleotide [$\Delta G_{(ATP)}$]. However, the efficiency of the energy conversion has been a matter of debate for over 50 years. In this study, with a highly reproducible analytical system using F_oF_1-ATP synthase from thermophilic *Bacillus*, apparently perfect energy conversion was observed. Mitchell's prediction thus has quantitative evidence.

Author contributions: N.S., K. Kinosita, M.Y., and T.S. designed research; N.S. and K. Kimura performed research; N.S. and T.S. analyzed data; and N.S., M.Y., and T.S. wrote the paper.

The authors declare no conflict of interest.

This article is a PNAS Direct Submission.

[1]Present address: Department of Applied Chemistry, Graduate School of Engineering, The University of Tokyo, Tokyo 113-8656, Japan.

[2]To whom correspondence should be addressed. Email: toshisuz@appchem.t.u-tokyo.ac.jp.

This article contains supporting information online at www.pnas.org/lookup/suppl/doi:10.1073/pnas.1700801114/-/DCSupplemental.

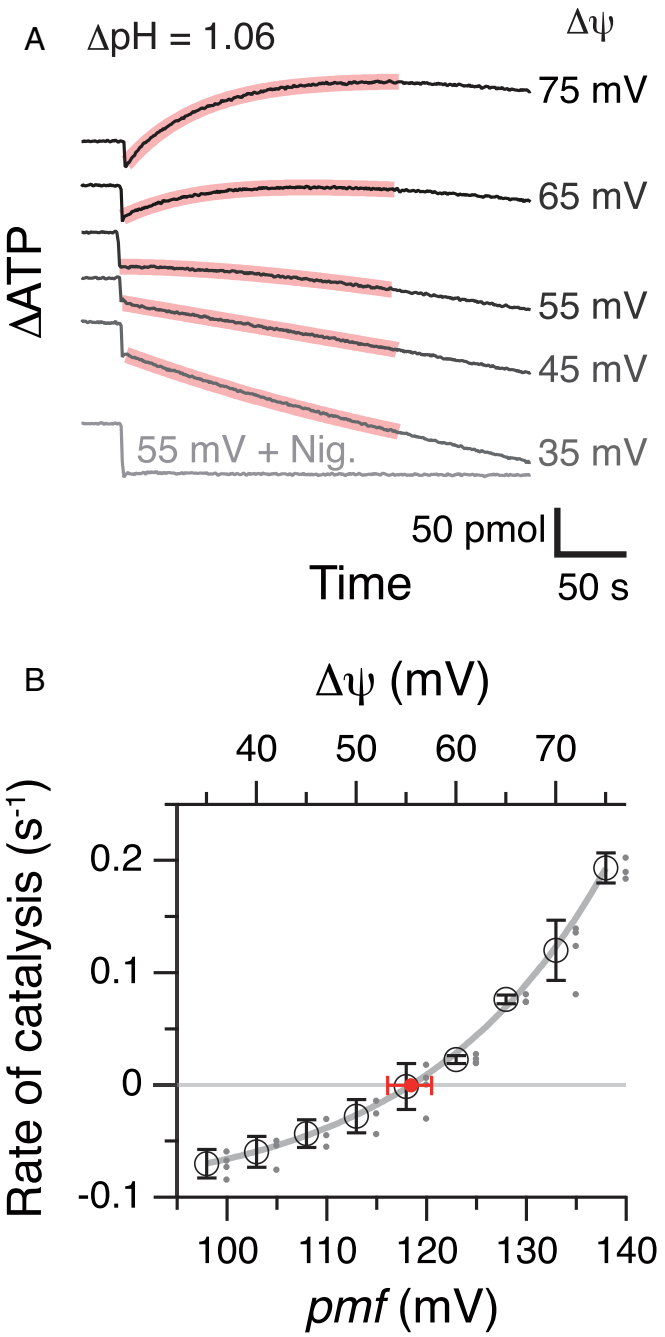

Fig. 1. ATP synthesis/hydrolysis at different *pmf* and determination of pmf_{eq}. (*A*) Typical time courses of ATP synthesis/hydrolysis at different *pmf*. Reaction was started by the injection of acidified PLs into the base medium containing luciferin/luciferase at $t = 0$. Vertical axis shows the amount of ATP in the reaction mixture quantified from the intensity of the luciferin luminescence. $K_{(ATP)}$ is 0.64; [ADP] = 80 μM, [Pi] = 10 mM, and [ATP] = 512 nM. ΔpH was 1.06 (pH_{out} 8.04 − pH_{in} 6.98), and Δψ was varied ($[K^+]_{in}$ = 5 mM; $[K^+]_{out}$ = 20–93 mM), giving 95 mV to 135 mV of *pmf*. Nigericine (500 nM) was added at Δψ of 55 mV. (*B*) The *pmf* dependency of ATP synthesis/hydrolysis and determination of pmf_{eq}. The initial rate of synthesis/hydrolysis was calculated from the exponential fit 0–200-s portions (red curves in *A*) and plotted against their *pmf* values. Experiments were repeated at least three times (dots beside the circle) and averaged (black open circles). The data points were fitted with an exponential function, and pmf_{eq} (red circle) was obtained at the point of rate = 0. An error bar of pmf_{eq} (red horizontal bar) was made from the fitting curves for the largest or the smallest rates at each *pmf*.

acidic medium, in which $[K^+]$ was 5 mM and pH was 6.98. In the following data analysis, $[K^+]_{in}$ is $[K^+]$ in the acidic medium, and pH_{in} is the actually measured pH of the acidified PLs solution. The reaction was initiated by rapid injection of the acidified PLs into a base medium containing luciferin, luciferase, and valinomycin. $[K^+]$ (20 mM to 93 mM) and actually measured pH (8.04) of the resulting reaction mixture correspond to $[K^+]_{out}$ and pH_{out}, respectively. By mixing, one unit of ΔpH (pH_{out} − pH_{in}) was established across membranes of the PLs. Transmembrane voltage, Δψ, generated by valinomycin-mediated diffusion potential of K^+, was calculated to be 35 mV to 75 mV by the Nernst equation based on the difference between $[K^+]_{out}$ and $[K^+]_{in}$. Change in [ATP] was monitored with luminescence from luciferin/luciferase system (Fig. 1*A*), and the initial rate of the change was obtained. The negative rates values correspond to hydrolysis of ATP by TF_oF_1. In the upper two traces, [ATP] reaches a plateau and then starts decreasing, reflecting that TF_oF_1 switches the direction of net catalysis from ATP synthesis to hydrolysis as *pmf* decays below pmf_{eq}. The magnitude of pmf_{eq} was obtained as 118 ± 2 mV from interpolation of the rate-vs.-*pmf* plot (Fig. 1*B*).

ATP Synthesis/Hydrolysis by TF_oF_1 at Various [ATP], [ADP], and [Pi]. Many series of measurements similar to those of Fig. 1 were carried out at different combinations of substrate concentrations (Tables S1 and S2). [ADP], [Pi], and [ATP] were varied in the range 20 μM to 640 μM, 0.1 mM to 10 mM, and 245 nM to 2,030 nM, respectively, and *pmf* ranging from 83 mV to 187 mV was imposed with 0.40, 1, or 1.64 units of ΔpH and 25 mV to 95 mV of Δψ (see also Fig. S1). The rate-vs.-*pmf* plots at 512 nM ATP and different [ADP] and [Pi] are shown in Fig. 2*A*, and those at different [ATP] are shown in Fig. 2 *B* and *C*. The traces are positioned roughly in parallel by the order of magnitudes of $K_{(ATP)}$. The pmf_{eq} and $K_{(ATP)eq}$ are obtained from each curve and used for the following analyses.

Tight Correlation Between Chemical Potential and *pmf*, and Determination of H^+/ATP Ratio. Both pmf_{eq} and $K_{(ATP)eq}$ were converted to the energy units of measurement (kilojoules per mole) according to the Eq. **5** and were plotted (Fig. 3*A*). All of the points fitted well to a linear function. A numerical value of the slope of the linear function gives the thermodynamic H^+/ATP ratios, n, and the y intercept of the function corresponds to the standard free energy of ATP synthesis, $\Delta G_p^{0'}$. The n value thus determined is 3.3 ± 0.1 (Fig. 3*B*). This value appears to be a perfect match with the c/β ratio of TF_oF_1 that is 10/3, indicating that TF_oF_1 achieves perfect coupling between downhill/uphill H^+ flow through F_o portion and ATP synthesis/hydrolysis in F_1 portion. The magnitude of $\Delta G_p^{0'}$ is estimated, from y intercept, to be 39 ± 1 kJ·mol^{-1}. Similar values are reported from the experiments of chloroplasts (36 ± 3 kJ·mol^{-1}) (14), yeast (36 ± 3 kJ·mol^{-1}) (15), and *E. coli* (38 ± 3 kJ·mol^{-1}) (16). Contamination of damaged TF_oF_1 in PLs that hydrolyzes ATP without H^+ pumping would be minimal. Even in the case where there is some contamination, the plots in Fig. 2 shift downward in parallel, making values of pmf_{eq} slightly larger, but the slope of the line in Fig. 3*A* remains almost the same whereas $\Delta G_p^{0'}$ becomes slightly larger.

Consideration of Possible Error in Δψ Estimation. In the above analysis, magnitude of Δψ was estimated from the Nernst equation. Possible error of the estimate was carefully discussed for experiments of chloroplast F_oF_1 by Turina et al. (18). As follows, we adhered to similar considerations in our case and verified that the main conclusion, H^+/ATP ratio = 3.3 ± 0.1, stands unaffected, although $\Delta G_p^{0'}$ becomes slightly smaller after the considerations. (*i*) The generation of the Δψ requires the flow of K^+ ions into PLs, and this flow induces the change in $[K^+]_{in}$. For example, when the maximum Δψ (95 mV, $[K^+]_{out}$ = 202 mM, $[K^+]_{in}$ = 5 mM) is induced by K^+

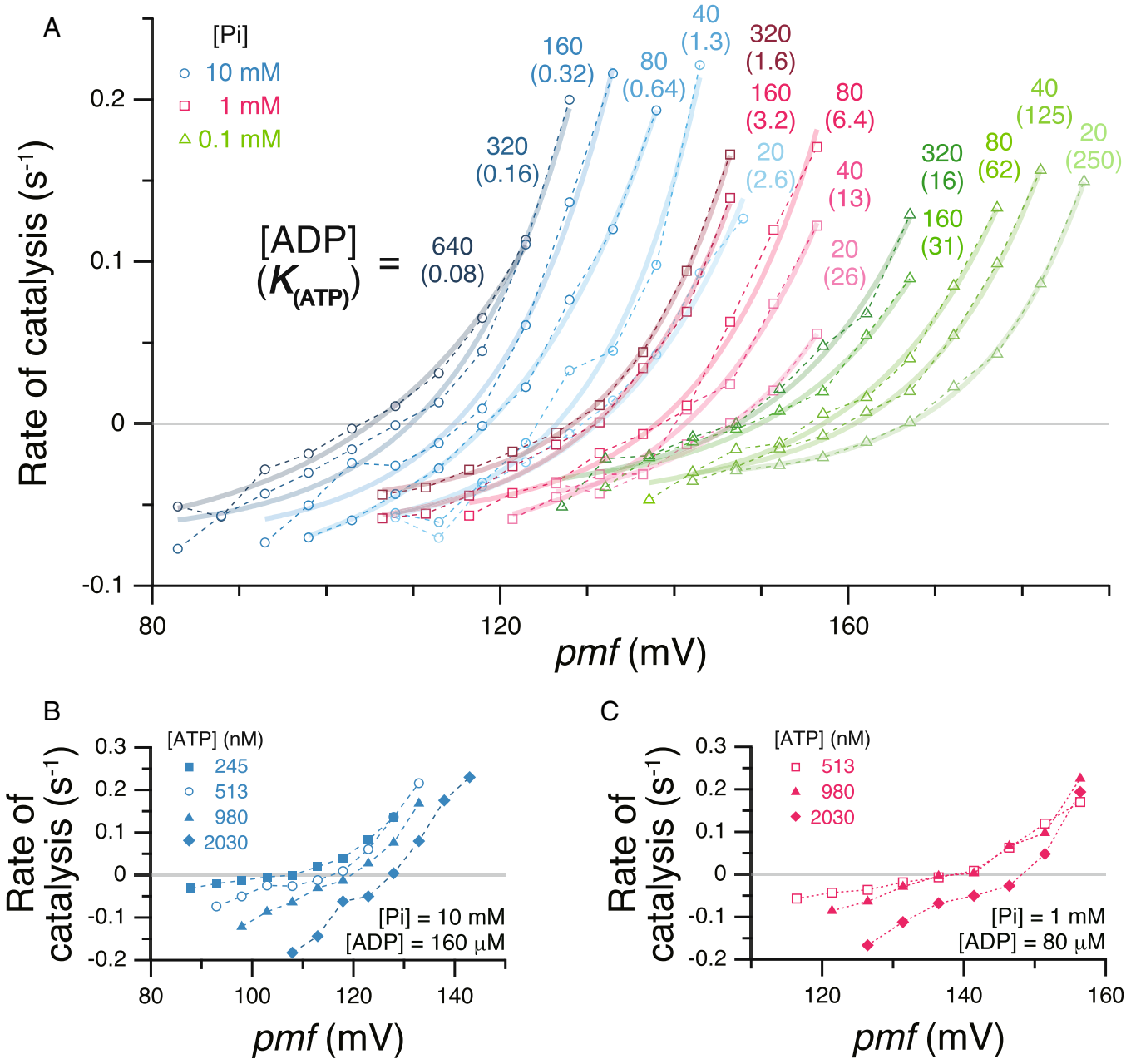

Fig. 2. The *pmf* dependency of ATP synthesis/hydrolysis at different $K_{(ATP)}$. (*A*) [ATP] = 512 nM. [Pi] = 10 mM (cyan circles), 1 mM (magenta squares), or 0.1 mM (green triangles). [ADP] and $K_{(ATP)}$ are shown on the top of each trace (the latter is in parentheses). (*B* and *C*) [ATP] was changed. [ATP], [ADP], and [Pi] are shown in the figure. Error bars are omitted for clarity (plots with error bars are shown in Fig. S1).

influx, the increase in $[K^+]_{in}$ is calculated to be 0.4 mM, taking into account membrane capacitance (~1 μF/cm^{-2}) and size of PLs (average diameter 170 nm). The change in $[K^+]_{out}$ is neglected because of the large volume of the solution outside of PLs. The increase in $[K^+]_{in}$ from 5.0 mM to 5.4 mM leads to generating weaker Δψ (93 mV) than in the case where K^+ influx is not assumed. Similarly, we recalculated $[K^+]_{in}$, Δψ, pmf_{eq}, and $K_{(ATP)eq}$ of all measurements, and generated a new plot (Fig. S2). The slope of the simulated line remains the same (H^+/ATP ratio = 3.3 ± 0.1) whereas $\Delta G_p^{0'}$ becomes slightly smaller (38 ± 1 kJ/mol). (*ii*) The proton efflux coupled with ATP synthesis (and by simple H^+ leak) leads to a charge compensating K^+ influx, and this influx changes $[K^+]_{in}$. The amount of K^+ influx caused by proton efflux was calculated under the condition where maximum ΔpH is applied (pH_{in} = 6.37, pH_{out} = 8.02, H^+/ATP-ratio = 3.3, time period = 5 s). It leads to 0.069 mM increase in $[K^+]_{in}$ at t = 5 s. The increase is over 70-fold smaller than the original $[K^+]_{in}$, 5 mM, and is negligible. (*iii*) By definition, the Nernst equation uses activities instead of concentrations of ion. Taking into account all inorganic ion species in the reaction mixtures, we estimated activities of K^+ according to the Debye–Huckel equation and calculated Δψ values with the Nernst equation using the activities of K^+. Then, new sets of $K_{(ATP)eq}$ and pmf_{eq} were obtained and plotted in Fig. S2. Compared with Fig. 3, the plots shifted slightly leftward in parallel, keeping the slope of the simulated line the same (H^+/ATP ratio = 3.3 ± 0.1). $\Delta G_p^{0'}$ became slightly smaller (37 ± 1 kJ/mol). Altogether, the error range of simple application of the Nernst equation to

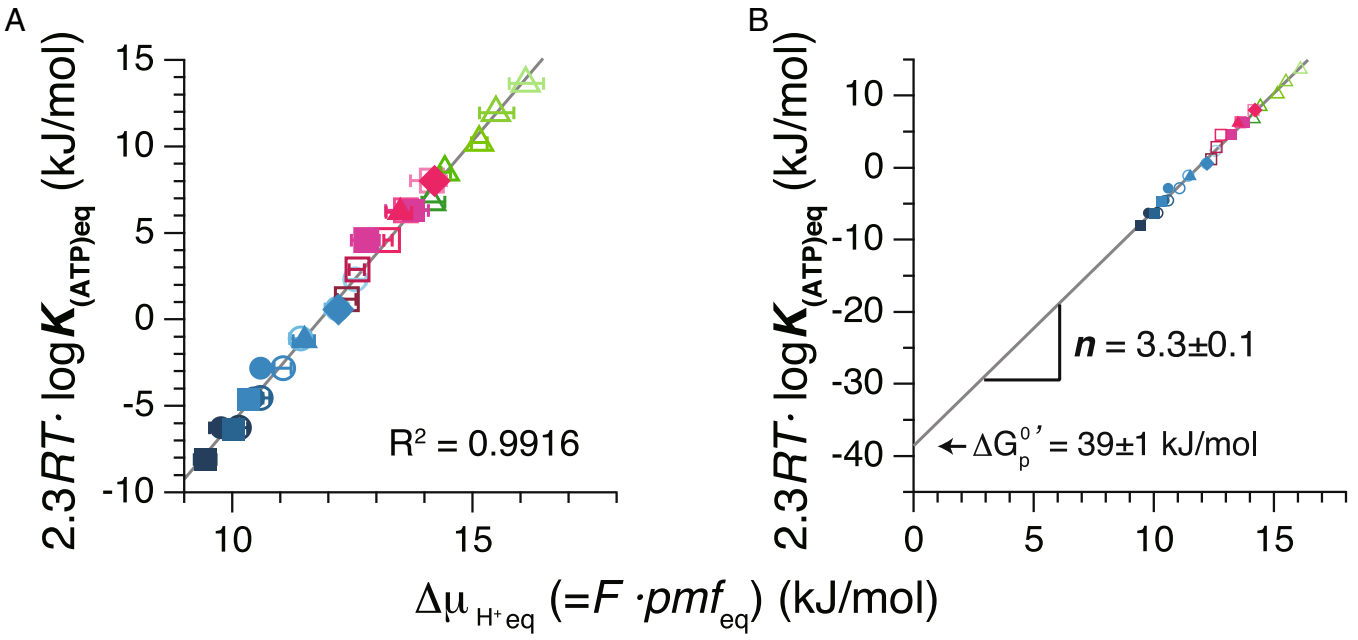

Fig. 3. Chemical potential of ATP synthesis at different electrochemical potentials of H^+ across membrane. (*A*) Chemical potential of ATP synthesis calculated from $K_{(ATP)eq}$ and electrochemical potential of H^+, $F{\cdot}pmf_{eq}$, of all datasets are shown. The plots were fitted with a linear function by the least squares method. The error bars in *A* were made as in Fig. 1*B*. (*B*) The trace in *A* is extrapolated to its *y* intercept region. From the slope and *y*-intercept point, *n* and $\Delta G_p^{0'}$ were determined as 3.3 ± 0.1 kJ/mol and 39 ± 1 kJ/mol.

estimate Δψ is very small and does not change the value of the H^+/ATP ratio.

Kinetic and Energetic Equivalence of ΔpH and Δψ. During this study, kinetic and energetic equivalence of two terms that define the energy of H^+ flow, ΔpH and Δψ, was confirmed with certainty. Their kinetic equivalence was previously reported (17), but this study demonstrates it under a wider range of conditions, including ATP hydrolysis. As shown (Fig. 4 *A*–*E*), a pair of experiments under the same conditions but a different combination of ΔpH and Δψ that gives the same *pmf* shows indistinguishable rate-vs.-*pmf* profiles. Energetic equivalence is obvious from Fig. 3*A* where energy for ATP synthesis/hydrolysis is defined solely by the value of *pmf* irrespective of the relative contribution of ΔpH and Δψ to *pmf*. When pairs with the same $K_{(ATP)eq}$ and pmf_{eq} are selected from all data, the difference in the relative ratio of the ΔpH and Δψ in the pmf_{eq} has no significant effect on the $K_{(ATP)eq}$ in each pair (Fig. 4*F*). This confirms the previous study of chloroplast F_oF_1 (18) that ΔpH and Δψ quantitatively contribute to *pmf* exactly as predicted by the established thermodynamic equation.

Discussion

H^+/ATP ratio is a key parameter of energy production of the cell and has been extensively investigated by using F_oF_1s of *E. coli*, yeast, and chloroplasts (14–16, 18). The studies have established valuable technique and theory, which enable us to make estimates of H^+/ATP ratio. The reported values of H^+/ATP ratios, however, did not fit the ratio of copy number of *c* subunit/β-subunit. In this report, we adopted and further optimized the procedures. Stable TF_oF_1 enabled us to develop a simple, unique method for PL preparation (17, 19), which does not use preformed liposomes as other studies did (14–16). PLs thus prepared are highly active and stable, allowing many measurements using the same PL preparation for several tens of hours, and give reproducible results (17). Measurements were repeated, and error bars of each result, as well as error range (±0.1) of the H^+/ATP ratio, are much smaller than those in the previous reports. Elimination of ATP contamination from commercial ADP down to 0.0005% also contributed significantly to setting accurate $K_{(ATP)}$ value, especially at high [ADP]. By virtue of these procedures that take advantage of the stable nature of TF_oF_1, the determined value of H^+/ATP ratio (3.3 ± 0.1) is now in close agreement with the *c*/β ratio (3.33...). A long-anticipated, but unproved, conception that F_oF_1 achieves a perfect coupling between transmembrane H^+ translocation and ATP synthesis/hydrolysis has direct experimental evidence now. A brief comment should be added concerning the reason why the values of H^+/ATP ratio of F_oF_1s of *E. coli* and chloroplasts do not match the *c*/β ratio. It was reported that chloroplast F_oF_1 needs activation by ΔpH and Δψ (18) and *E. coli* F_oF_1 needs activation by Δψ (20). The maximum rate of ATP synthesis by *E. coli* F_oF_1 is limited by the magnitude of Δψ. It is possible that their measurements were accurate but that these regulatory activation processes could cause deviation of the observed H^+/ATP ratio from the *c*/β values.

In a thermodynamic view, the perfect coupling means perfect energy conversions between chemiosmotic (H^+ translocation), mechanical (rotary motion), and chemical energy (ATP synthesis/hydrolysis). A near-perfect energy conversion from ATP hydrolysis to rotary motion of γ-subunit in F_1 was recently demonstrated in a thermodynamically defined manner (21), and this study predicts that other conversions should also be highly efficient. In a mechanistic view, the perfect coupling means that there is no slippage within and between F_o motor and F_1 motor. Atomic structures of F_1 are convincing that rotary motion of the γ-subunit could not occur without conformation change of the catalytic subunits. Structural basis for rotation of F_o motor without slippage has been suggested recently by atomic structures of whole F_oF_1 revealed by cryoelectron microscopy (22). The connection of the two motors should also be strong enough to endure the twisting force of torque. Crystal structures of F_1·*c*-ring complexes indicate that the connection appears to be held by a small number of interactions between the bottom portion of F_1's rotor and polar loops in the *c* ring (11). Interestingly, this connection must be versatile, because the chimera TF_oF_1 with

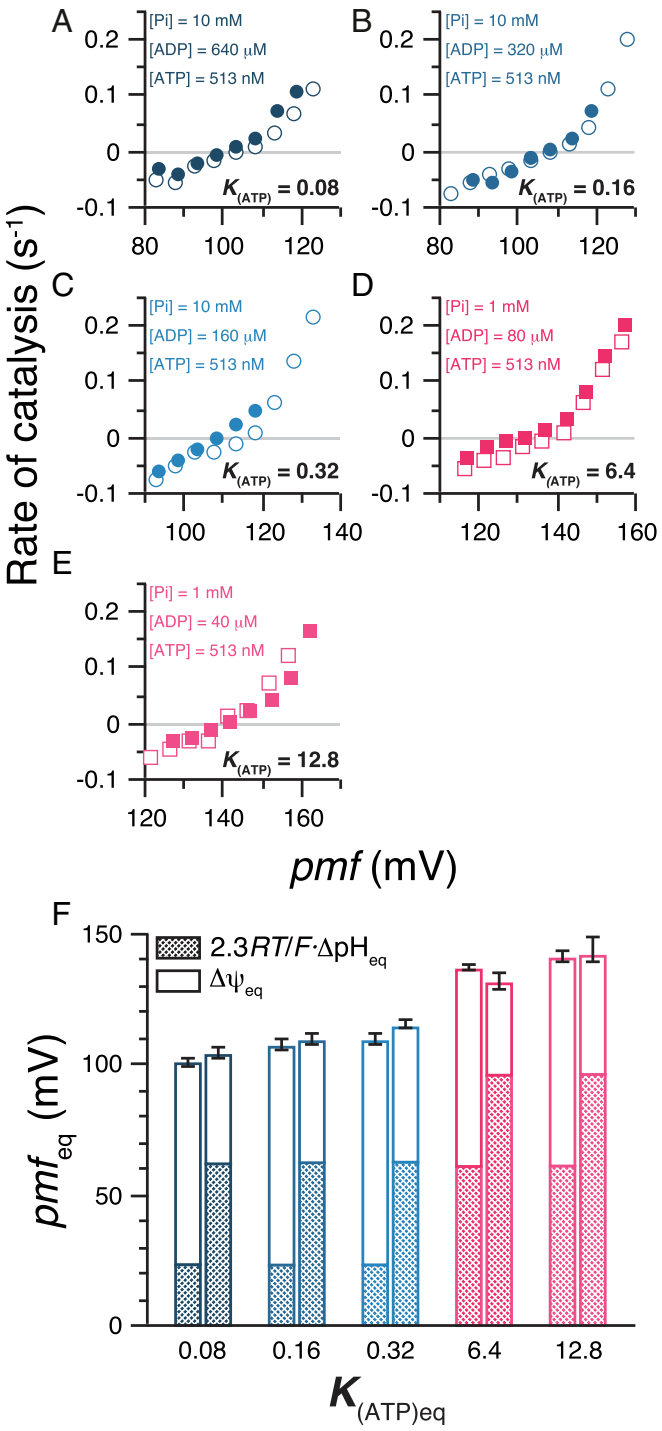

Fig. 4. Equivalent contribution of ΔpH and Δψ to ATP synthesis/hydrolysis. (*A*–*E*) Kinetic equivalence of ΔpH and Δψ. A pair of rate-vs.-*pmf* plots under the same conditions except different combinations of ΔpH and Δψ that gives the same *pmf*. [ATP], [ADP], and [Pi] are indicated. ΔpH was set to 1.04 or 1.06 (open circles and open squares in *A*–*E*), 0.40 (filled circles in *A*–*C*), and 1.64 units (filled squares in *D* and *E*), and Δψ was changed by changing $[K^+]_{out}$. Error bars are omitted for clarity. (*F*) Thermodynamic equivalence of ΔpH and Δψ terms. Pairs of datasets with the same $K_{(ATP)eq}$ and pmf_{eq} were selected, and contributions of Δψ and ΔpH in each dataset (bar) are shown with opened and meshed areas, respectively. Colors of the bars are same as those in *A*–*E*. Detailed conditions of the measurements are summarized in Tables S1 and S2.

replaced F_o from *Propionegenium modestum* (23) that has 11 *c* subunits shows good coupled activity.

Materials and Methods

Chemicals. ATP, ADP, valinomycin, and Pi were purchased from Sigma (A2383, A2754, and V0627) and Wako Pure Chemical (198-14505). As the commercial ADP contained ~0.05% ATP contamination (molar ratio), the contaminated ATP was eliminated by anion exchange column chromatography (MonoQ 5/50 GL; GE Healthcare) as follows: After loading 4 mL of 20 mM ADP dissolved in 10 mM Tricine/NaOH (pH 8.03), the column was washed with the buffer, and ADP was eluted with the buffer supplemented with 150 mM NaCl. Only the initial 1.5 mL of the ADP peak was collected. ATP contamination in the purified ADP solution decreased 100-fold (0.0005% ATP relative to ADP). Contamination of Pi in the reaction mixture used for measurement of the catalytic activity was quantified to be 3 μM by EnzCheck phosphate assay kit (Thermo Fischer).

Preparation of F_oF_1, Lipids, and PLs. A mutated F_oF_1 of *Bacillus* PS3, F_oF_1-εΔc (17, 19, 24), was used throughout this study. The F_oF_1 has a histidine tag composed of 10 histidine residues at N terminus of β and lacks C-terminal domain of the ε subunit, of which the mutations have no significant effect on catalytic function (17, 24). The mutated F_oF_1 is named as just TF_oF_1 in this paper. TF_oF_1 was overexpressed in F_oF_1-deficient *E. coli* strain DK8 using plasmid pTR19-ASDS-εΔc. Preparation of membrane fraction and purification of TF_oF_1 were performed as described previously (17).

Lipid and PLs reconstituted with TF_oF_1 were prepared by the methods in ref. 17, with a modification: for preparation of PLs, dioleoyl L-α-phosphatidylethanolamine (Wako Pure Chemical Industries) was supplemented at a final concentration of 4 mg/mL to 36 mg/mL (5 mM) of the soybean lipid that was previously washed repeatedly to eliminate contamination of K^+ ions (17). Contamination of uncoupled TF_oF_1 in PLs was minimal because ATP hydrolysis activity of PLs was inhibited nearly completely (92 to 98% inhibition) by a proton translocation inhibitor, dicyclohexylcarbodiimide.

Measurement of ATP Synthesis/Hydrolysis Activity and Data Analysis. Measurement of ATP synthesis/hydrolysis activity was performed using the method of acid/base transition with valinomycin-induced Δψ, as described previously (17). Briefly, PLs were acidified as follows: 30 μL of the PLs (40 mg lipid per milliliter) was mixed with 70 μL of acidification buffer (40 mM buffer containing 0.147 mM to 14.7 mM NaH_2PO_4, 6 mM $MgCl_2$, 5 mM KCl, 4 mM NaCl, 0.5 M sucrose, 0.03 mM to 0.9 mM purified ADP, 0.04 μM to 3 μM ATP, and 0.3 μM fresh valinomycin), and pH was adjusted with NaOH. The mixture was incubated for 10 h to 20 h at 23 °C to 27 °C to acidify inside PLs. Base medium was prepared by mixing 25 μL of the luciferin/luciferase mixture (2× concentration of CLSII solution in ATP bioluminescence assay kit; Roche) supplemented with 5 mM luciferin (L9504; Sigma), 800 μL of base buffer (350 mM Hepes, 11.3, 1.13, or 0.113 mM NaH_2PO_4, 5.6 mM $MgCl_2$, 5.6 mM KCl, 11.25 mM NaCl, and 272 mM mixture of KOH + NaOH to keep total concentration of Na^+ plus K^+ in the solution), 18 μL of 1 mM to 32 mM ADP, and 57 μL of water. Details of the acidification buffer and base medium are summarized in Table S1. For the assay, base medium (900 μL) was incubated at 25 °C for 8 min for equilibrium. The catalytic reaction, ATP synthesis and hydrolysis, was initiated by injecting 100 μL of the acidified PLs suspension into the base medium (time $t = 0$ s). The final TF_oF_1 concentration was 8.5 nM. This acid–base transition should lead to transmembrane fluxes of all permeable ions, but, by the assist of valinomycin, K^+ ions are selectively and efficiently transported into PLs several orders of magnitude faster than all other ions, and diffusion potential of K^+ ion is established instantaneously. Change in the ATP concentration was monitored in real time by luminescence light from luciferin/luciferase using a luminometer (Luminescencer AB2200 with sample injection apparatus; ATTO). Upon injection, the intensity of luminescence showed a negative jump. Magnitude of the jump fluctuated from one measurement to another for unknown reasons, but the luminescence intensity per unit amount of ATP calibrated in each measurement was reproducible. Initial ATP concentration at $t = 0$ was obtained from the light intensity just after the negative jump. At $t = 200$ s, 10 μL of 10 μM ATP was added three times for calibrating luminescence light intensity to ATP concentration. Maximum ATP concentration measurable by this luciferin/luciferase method is ~2 nmol/mL. The initial rate at 0 s was calculated by regression analysis of the time courses (0 s to 200 s) with sum of a single-exponential function and linear function (14). All experiments we performed contribute to the statistics (every point in the graphs shows the average over at least three measurements using three or more independent preparations of PLs, and the error bar indicates the SD). The pH_{in} and pH_{out}

were determined by directly measuring pH, respectively, of the acidified PLs solution and of reaction mixture (base medium supplemented with acidified PLs) for every condition using the same glass electrode. ΔpH was obtained by subtracting pH_{in} from pH_{out}. Transmembrane electrical potential, Δψ, was calculated using the Nernst equation, $\Delta\psi = 2.3RT/F\log([K^+]_{out}/[K^+]_{in}) = 59.1\cdot\log([K^+]_{out}/[K^+]_{in})$, where $[K^+]_{in}$ and $[K^+]_{out}$ were K^+ concentrations in the acidification buffer containing PLs and in the reaction mixture after adding acidified PLs, respectively. As carefully examined in our previous report (figure S4 of ref. 17), when $[K^+]_{in}$ is above 1 mM, initial rates of TF_oF_1-catalyzed ATP synthesis are consistently simulated by a function of *pmf*, in which Δψ is estimated from the Nernst equation. However, they start to show some deviation from the function when $[K^+]_{in}$ is deceased below 1 mM. In the present study, $[K^+]_{in}$ was fixed to 5 mM in all experiments, and the Nernst equation should be valid for estimation of Δψ values.

Functions and Calculations. Determination of $K_{(ATP)eq}$, pmf_{eq}, and n was performed as follows. In Peter Michel's chemiosmotic coupling theory (1), ATP synthesis/hydrolysis catalyzed by F_oF_1-ATP synthase should be coupled with translocation of n protons, in which n is the required number of protons in a single ATP catalysis reaction,

$$ADP + Pi + nH^+_{in} \rightleftharpoons ATP + H_2O + nH^+_{out}. \quad [1]$$

The Gibbs free energy of the coupled reactions, $\Delta G'$, is expressed by

$$\begin{aligned}\Delta G' &= \Delta G'_p - n\Delta\tilde{\mu}_{H^+}\\ &= \Delta G'_p - n(2.3RT\Delta pH + F\Delta\psi)\\ &= \Delta G'_p - nF\cdot pmf,\end{aligned} \quad [2]$$

where ΔG_p is the Gibbs free energy of ATP synthesis, and $\Delta\tilde{\mu}_{H^+}$ is the transmembrane electrochemical potential difference of the proton, which can be converted to proton motive force (referred to as *pmf* in this study) in millivolts comprising transmembrane difference of pH, $\Delta pH = pH_{out} - pH_{in}$, and transmembrane difference of electrical potential, $\Delta\psi = \psi_{in} - \psi_{out}$, and R, T, and F are gas constant, absolute temperature, and Faraday constant, respectively. The Gibbs free energy of ATP synthesis, $\Delta G^{0'}_p$, is given by

$$\Delta G'_p = \Delta G^{0'}_p + 2.3RT\cdot\log\frac{[ATP]c^0}{[ADP][Pi]} = \Delta G^{0'}_p + 2.3RT\cdot\log K_{(ATP)}, \quad [3]$$

where $\Delta G^{0'}_p$ is the Gibbs free energy at the biochemical standard state, c^0 is the standard concentration (equal to 1M), and $K_{(ATP)}$ is a ratio, [ATP]/([ADP]·[P_i]. Therefore, Eq. **4** is obtained by the sum of Eqs. **2** and **3**,

$$\Delta G' = \Delta G^{0'}_p + 2.3RT\cdot\log K_{(ATP)} - nF\cdot pmf. \quad [4]$$

At the energetic equilibrium point of the coupled reactions ($\Delta G' = 0$), Eq. **4** can be converted to

$$2.3RT\cdot\log K_{(ATP)eq} = -\Delta G^{0'}_p + nF\cdot pmf_{eq}, \quad [5]$$

in which pmf_{eq} is a variable and experimentally measurable value. Therefore, with data sets of $K_{(ATP)eq}$ and its corresponding pmf_{eq}, $\Delta G^{0'}_p$ and n can be determined by the linear regression analysis.

ACKNOWLEDGMENTS. We thank Mr. C. Wakabayashi (Japan Science and Technology Agency) for continuous support in TF_oF_1 purification, Dr. M. Bertz (Waseda University) for an analysis program, Drs. Y. Kasuya (Waseda University), H. Noji (The University of Tokyo), and R. Watanabe (The University of Tokyo) for discussion, members in the K. Kinosita and M.Y. laboratories for help and advice, and S. Takahashi for encouragement and laboratory management. We also thank Dr. B. A. Feniouk (Moscow State University) for advice and detailed discussion throughout this study. This work was supported by Grants-in-Aid for Specially Promoted Research (to K. Kinosita), Research Fellow (to N.S.) and Scientific Research (to T.S.) of Japan Society for the Promotion of Science; and by the ATP synthesis Regulation Project organized by Japan Science and Technology Agency (M.Y.).

1. Mitchell P (1966) Chemiosmotic coupling in oxidative and photosynthetic phosphorylation. *Biol Rev Camb Philos Soc* 41:445–502.
2. Yoshida M, Muneyuki E, Hisabori T (2001) ATP synthase–A marvellous rotary engine of the cell. *Nat Rev Mol Cell Biol* 2:669–677.
3. Weber J, Senior AE (2000) ATP synthase: What we know about ATP hydrolysis and what we do not know about ATP synthesis. *Biochim Biophys Acta* 1458:300–309.
4. Senior AE, Nadanaciva S, Weber J (2002) The molecular mechanism of ATP synthesis by F_1F_0-ATP synthase. *Biochim Biophys Acta* 1553:188–211.
5. Noji H, Yasuda R, Yoshida M, Kinosita K, Jr (1997) Direct observation of the rotation of F_1-ATPase. *Nature* 386:299–302.
6. Itoh H, et al. (2004) Mechanically driven ATP synthesis by F_1-ATPase. *Nature* 427: 465–468.
7. Rondelez Y, et al. (2005) Highly coupled ATP synthesis by F1-ATPase single molecules. *Nature* 433:773–777.
8. Seelert H, et al. (2000) Structural biology. Proton-powered turbine of a plant motor. *Nature* 405:418–419.
9. Vollmar M, Schlieper D, Winn M, Büchner C, Groth G (2009) Structure of the c_{14} rotor ring of the proton translocating chloroplast ATP synthase. *J Biol Chem* 284: 18228–18235.
10. Watt IN, Montgomery MG, Runswick MJ, Leslie AG, Walker JE (2010) Bioenergetic cost of making an adenosine triphosphate molecule in animal mitochondria. *Proc Natl Acad Sci USA* 107:16823–16827.
11. Stock D, Leslie AG, Walker JE (1999) Molecular architecture of the rotary motor in ATP synthase. *Science* 286:1700–1705.
12. Mitome N, Suzuki T, Hayashi S, Yoshida M (2004) Thermophilic ATP synthase has a decamer *c*-ring: Indication of noninteger 10:3 H^+/ATP ratio and permissive elastic coupling. *Proc Natl Acad Sci USA* 101:12159–12164.
13. Jiang W, Hermolin J, Fillingame RH (2001) The preferred stoichiometry of *c* subunits in the rotary motor sector of *Escherichia coli* ATP synthase is 10. *Proc Natl Acad Sci USA* 98:4966–4971.
14. Turina P, Samoray D, Gräber P (2003) H^+/ATP ratio of proton transport-coupled ATP synthesis and hydrolysis catalysed by CF_0F_1-liposomes. *EMBO J* 22:418–426.
15. Petersen J, Förster K, Turina P, Gräber P (2012) Comparison of the H^+/ATP ratios of the H^+-ATP synthases from yeast and from chloroplast. *Proc Natl Acad Sci USA* 109: 11150–11155.
16. Steigmiller S, Turina P, Gräber P (2008) The thermodynamic H^+/ATP ratios of the H^+-ATPsynthases from chloroplasts and *Escherichia coli*. *Proc Natl Acad Sci USA* 105: 3745–3750.
17. Soga N, Kinosita K, Jr, Yoshida M, Suzuki T (2012) Kinetic equivalence of transmembrane pH and electrical potential differences in ATP synthesis. *J Biol Chem* 287: 9633–9639.
18. Turina P, Petersen J, Gräber P (2016) Thermodynamics of proton transport coupled ATP synthesis. *Biochim Biophys Acta* 1857:653–664.
19. Soga N, Kinosita K, Jr, Yoshida M, Suzuki T (2011) Efficient ATP synthesis by thermophilic *Bacillus* F_oF_1-ATP synthase. *FEBS J* 278:2647–2654.
20. Fischer S, Gräber P (1999) Comparison of ΔpH- and Δϕ-driven ATP synthesis catalyzed by the H^+-ATPases from *Escherichia coli* or chloroplasts reconstituted into liposomes. *FEBS Lett* 457:327–332.
21. Saita E, Suzuki T, Kinosita K, Jr, Yoshida M (2015) Simple mechanism whereby the F_1-ATPase motor rotates with near-perfect chemomechanical energy conversion. *Proc Natl Acad Sci USA* 112:9626–9631.
22. Allegretti M, et al. (2015) Horizontal membrane-intrinsic α-helices in the stator *a*-subunit of an F-type ATP synthase. *Nature* 521:237–240.
23. Suzuki T, Ozaki Y, Sone N, Feniouk BA, Yoshida M (2007) The product of *uncI* gene in F_1F_o-ATP synthase operon plays a chaperone-like role to assist *c*-ring assembly. *Proc Natl Acad Sci USA* 104:20776–20781.
24. Konno H Suzuki T, Bald D, Yoshida M, Hisabori T (2004) Significance of the epsilon subunit in the thiol modulation of chloroplast ATP synthase. *Biochem Biophys Res Commun* 318:17–24.